Research Article

An Advanced Method to Voxelize a Tissue Using CT Scan Images and Medical Imaging

S. A. Mousavi Shirazi [a]

a Department of Physics, South Tehran Branch, Islamic AZAD University, Tehran, Iran.

*Corresponding Author Email: alireza.mousavishirazi@gmail.com

ABSTRACT   Received: Oct. 24, 2024, Revised: Jan. 7, 2025, Accepted: Jan. 26, 2025, Available Online: Feb. 17, 2025

This study focused on medical imaging for X-ray radiotherapy. To conduct the research, liver tissue was outlined using CT images of the abdominal area. The precise geometry of the segmented liver tissue was then simulated and created with specialized medical imaging software. Initially, the Hounsfield Unit for each tissue type in the body was determined, followed by defining the constituent materials, which were then input into MATLAB code. Next, based on its radiodensity, the abdominal tissue was uniformly filled with the appropriate material. Subsequently, the liver tissue was outlined and segmented within the abdominal tissue, and the precise geometry of the segmented liver tissue was created as input data. This approach can be applied to any patient using their individual CT scan images.

I. INTRODUCTION

The initiation of advanced tomographic and computer imaging methods in the late 1980s marked the beginning of a novel era for VOXEL phantoms [1].

In radiotherapy, there is a need to minimize the dose delivered to healthy tissues. Simultaneously, accurately measuring and evaluating the absorbed dose is of primary importance [2, 3]. X-ray photon-based cancer therapy is a commonly used treatment method in medical radiation. This study aimed to develop medical imaging techniques that can be utilized in dosimetry to examine the behavior of beams in tissues. To validate the effectiveness of the developed imaging, a dosimetric approach was applied to real tissue using DICOM images from computed tomography (CT) scans [4, 5].

The current technologies still have many critical limitations. The voxelization process itself demands a substantial amount of computational power, which limits the use of current technologies. Some tissues lack reference values, such as the skin, gallbladder wall, major blood vessels, bronchi, and adipose

tissue. Modeling very thin structures, like the oral mucosa skin, and bone endosteum, crucial for radiation protection, is practically impossible. Using extremely small VOXELs for such thin structures needs an enormous amount of computer memory, and the computation process is very slow [6, 7].

A significant advancement came with the advancement of CT and magnetic resonance imaging (MRI), which are capable of producing highly accurate digital 3D images of internal organs. In the VOXEL model, diagnostic data is converted into a volumetric pixel format, enabling the recreation of the human body in digital 3D form. To achieve this, raw data from CT or MRI scans must be obtained, and the body's components need to be segmented and separated from other tissues [8]. Each component's density and composition must be determined, and this information must be incorporated into a unified 3D structure [9, 10]. Additionally, the majority of scans of a single subject capture merely a body's small section, while a series of full scans is required to obtain meaningful data. Managing this data can be challenging [11]. During a Monte Carlo simulation, it is impossible to deform or move the phantom internal organs, which necessitates precise modeling of organs in simulations (such as for imaging of moving organs, 4D radiotherapy, and radiation therapy). This represents a significant restriction [12].

II. MATERIALS AND METHODS

The CT scan images of the abdominal tissue of a 45-year-old man were obtained by 80 keV photons from the single direction at the Cartesian coordinates, which were viewed from the XZ direction, showing the liver ventral view.

In this research, 85 DICOM images were selected from the YZ axes in the Cartesian coordinates to allow for the observation of the front view of the tissue.

A large lattice is defined in such a way that it can be subdivided into highly small lattices using specialized software. Their resolution can be adjusted as needed. Their resolution was set to 1mm3. Every volume made by this program plays the role of one VOXEL. Every VOXEL is completely homogenous and filled up using the related matter (abdominal tissue matters) which has self-density. Then, these VOXELs cover all the abdominal tissue. While the abdominal tissue contains liver tissue, contouring the liver tissue and separation of its slices are very difficult.

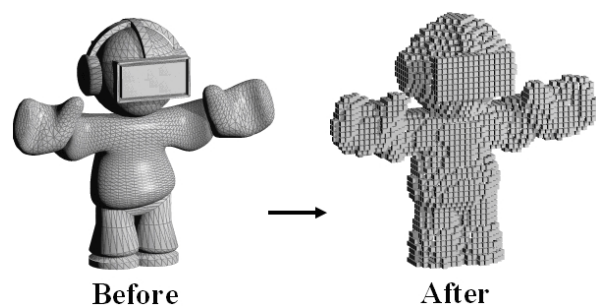The related figures have been illustrated as follows [13, 14].

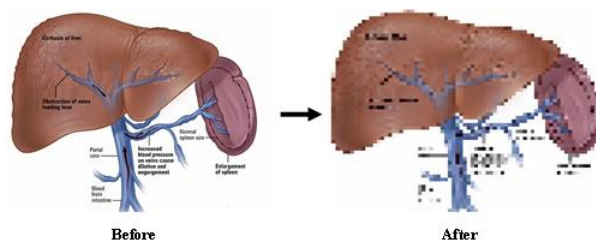Fig. **1** The image of a manikin before and after voxelization

Fig. **2** The image of the liver before and after voxelization

Some of the requirements in the VOXEL model are as follows:
1- Requiring the individual organ topology, 2- Requiring the individual organ masses, 3- knowing the values of tissues.

In this investigation, the contoured shape of liver tissue has been considered. Following voxelization and filling the abdominal tissue using appropriate compounds, the liver tissue

underwent contouring and segmenting within the abdominal area.

This contouring process involves filling the remaining materials in other tissues and sections of the abdomen with air.

The VOXEL phantom can be typically described as a rectangular array of VOXELs containing only the body region along with some surrounding air [15].

Since the rectangular array is treated as one entity, it is challenging or nearly impossible with most software to define an organ near its region unless it is inserted and voxelized within that area. The surrounding air regions can be reduced to represent the VOXEL region instead of using a rectangular array, but those regions cannot be eliminated. The VOXEL phantom limitations also pose considerable challenges in proton beam treatment simulations, in which the beam nozzle and other equipment should be modeled near the body region [16, 17, 18].

The scanned images (slices) are then processed into new images using specific MATLAB programming.

This program generates numerous volumes as lattices, with each lattice being repeated to construct the complete geometry of the tissue. Each material, such as air, water, soft, bone, etc., has its radiodensities. Then, these VOXELs cover all the abdominal tissue.

The type of each material is determined using the Hounsfield Unit (HU) scale of DICOM CT slices. Each pixel in the slices corresponds to one voxel, establishing a correlation between the HU and each voxel. Therefore, the existing voxels in the abdominal tissue are identified using MATLAB software, which analyzes the grayness level of the CT slice along with its associated HU. Each tissue in the abdominal area is described based on the HU considering the following equation [19, 20].

$$HU = \frac{\mu_X - \mu_{water}}{\mu_{water} - \mu_{air}} \times 1000 \qquad (1)$$

Where:

μ_{water}: water linear attenuation coefficient.

μ_X: linear attenuation coefficient for a material X.

μ_{air}: air linear attenuation coefficient.

The HU values related to some other body tissues are calculated for the MATLAB programming based on their HU calculations and through their μX, and they are added to the prior-defined materials.

There are the radiodensities of materials existing in the liver tissue defined based on HU for each cell. As every VOXEL has a self-CT number, each radiodensity is accurately associated with that of the cell. However, every VOXEL will have its related radiodensity [21].

The HU values and μ for some body tissues can be shown for MATLAB programming according to Tables 1 and 2, respectively.

TABLE. **1** THE HU VALUES FOR DIFFERENT BODY TISSUES APPLIED FOR MATLAB PROGRAMMING [22]

Tissue	HU values
Air	-1000
Fat	-100
Breast	-150
Lung	-880
Muscle	100
Liquid	-2
Soft	1
Water	0
Aluminum	2640
Bone	400

TABLE. **2** LINEAR ATTENUATION COEFFICIENT VALUES (CM⁻¹) RELATED TO SELECT TISSUES AT VARIOUS X-RAY PHOTON ENERGIES [23]

Tissue (material)	40 keV	60 keV	80 keV	100 keV
Fat	0.228	0.188	0.171	0.160
Water	0.268	0.206	0.184	0.171
Bone	1.28	0.604	0.428	0.356
Aluminum	1.535	0.750	0.545	0.460
Titanium	10.05	3.48	1.840	1.235

To accurately identify the initial slice of the DICOM CT scan where the liver tissue begins, a reference point must be established using DICOM images from three perspectives in

Cartesian coordinates (XY, YZ, and XZ). Assuming the cancerous tumor in the liver tissue for tumor contouring, the DICOM CT slices are analyzed starting from the point where the tumor becomes visible at the end of its depth.
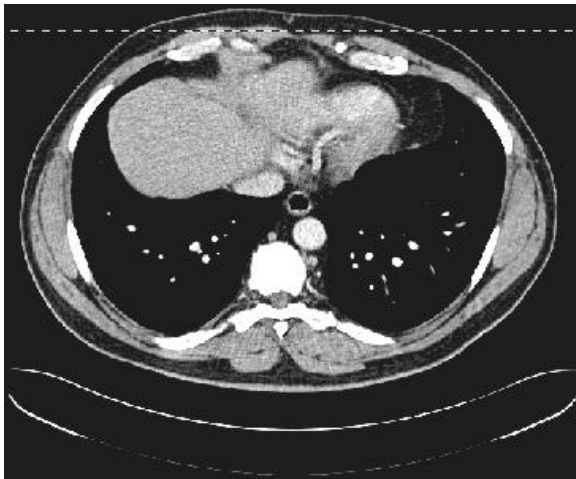

Fig. **3** Slice No. 36 of 237 CT slices from XZ direction through holding slice No. 18 in XY direction
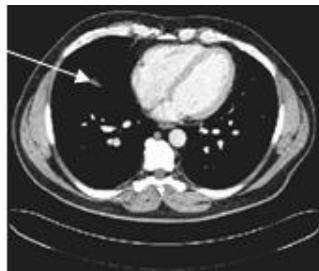

Fig. **4** Slice No. 13 of 237 CT slices in the XZ direction.

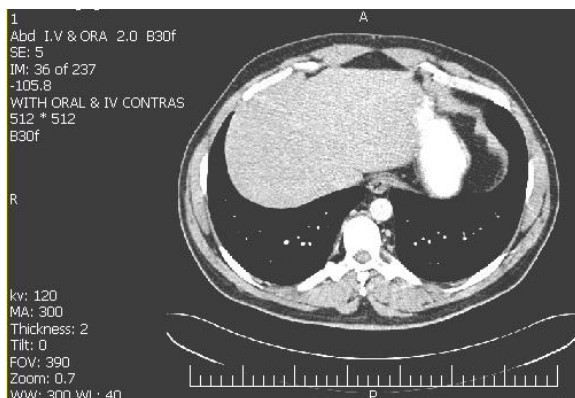Fig. **5** The image of abdominal tissue's slice by CT scanning from an X-Z view

This specific program plays a significant role in converting the images scanned by CT scanning equipment into the inputting data of MCNPX

code in a way that all the liver geometry is defined from CT imaging to the inputting data of MCNPX code. It means the liver geometry is finally described from CT imaging into inputting data of MCNPX code; thereby simulation of a real liver tissue is done.

Finally, for the sake of dose calculation, at this time, the materials existing in the liver tissue are described as input for the MCNPX Code, the MCNPX programming is run, and the precise absorbed doses are finally achieved. In that case, every part of the abdominal tissue is automatically colored by the MCNPX code based on the material number.

III. RESULTS AND DISCUSSION

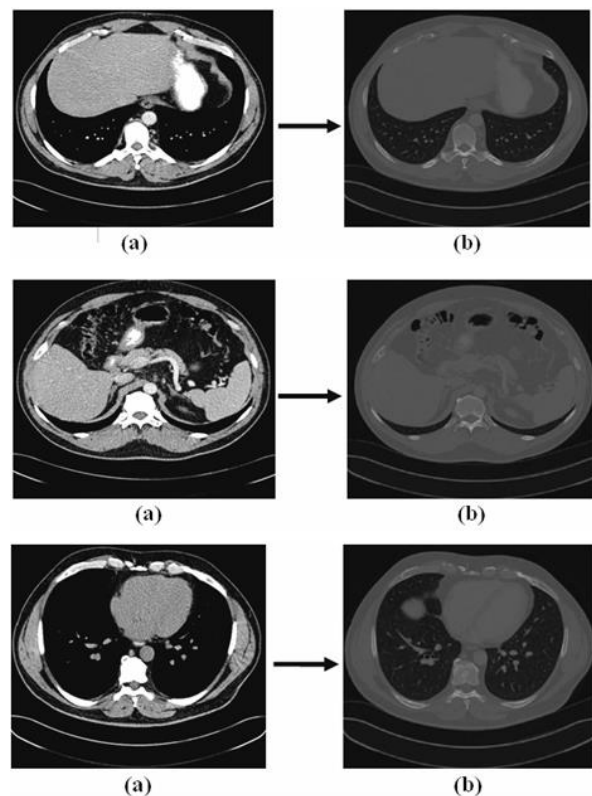Some abdominal region plots, converted using MATLAB, were consecutively shown in two steps (Figure 6).

Fig. **6**(a) Image of abdominal tissue slice by CT scanning (b) Image of abdominal tissue converted using MATLAB from CT image

The total absorbed dose amount in the liver tissue is illustrated in Fig 7:
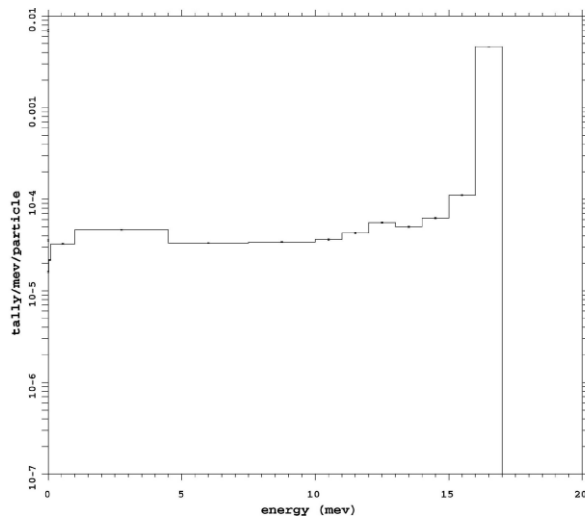
Fig. **7** The overall absorbed dose in the segmented liver tissue using liver voxelization (plotted using MCNPX code)

In another section, abdominal tissue DICOM images were used. Using MATLAB and these DICOM images, the abdominal tissue-surrounded liver tissue was isolated followed by irradiation using photon-X, comparable to the liver phantom.

IV. CONCLUSIONS

It was concluded the method presented in this research can be applied for radiation dosimetry for patients undergoing various radiotherapy courses, such as Boron Neutron Capture Therapy (BNCT). Additionally, it can be widely implemented for different types, forms, and sizes of tissues. This imaging method can also be used for dosimetric purposes and to analyze the behavior of radiation beams within liver tissue components. DICOM images are adaptable for any body tissue, making it easier to consider a cancerous mass or tumor in the liver tissue and break down its constituent elements. When applying DICOM images from CT scans in dosimetry, this approach is applicable for each case using their own CT scan images to calculate the allowable equivalent and absorbed doses, after the procedures outlined.

By applying this method, the precise absorbed dose can be calculated in the whole of a tissue and its constituent elements in radiotherapy as accurately as possible.

Therefore, the advantage of this method is that it can be personalized for each patient using their own CT scans to determine the acceptable absorbed dose, and all the procedures described in this study can be applied. Additionally, this method could be extended to other radiotherapies, such as proton or photon treatments.

REFERENCES

[1] Kramer R, Cassola V.F, Khoury H.J, Vieira J.W, de Melo Lima V.J, and Brown K.R, "FASH and MASH: female and male adult human phantoms based on polygon mesh surfaces: II. Dosimetric calculations," Physics in medicine & biology. vol. 55, pp.163, 2009.

[2] Reginatto M. "What can we learn about the spectrum of high-energy stray neutron fields from Bonner sphere measurements," Radiation Measurements. vol. 44, pp. 692-699, 2009.

[3] Morris S, Roques T, Ahmad S, and Loo S, *Practical radiotherapy planning.* CRC Press, 2023.

[4] Shirazi S.A and Shafeie Lilehkouhi M.S. "The assessment of radioisotopes and radiomedicines in the MNSR reactor of Isfahan and obtaining the burnup by applying the obtained information," Asia-Pacific Power and Energy Engineering Conference, vol. , pp. 1-4, 2012.

[5] Mousavi Shirazi S.A and Rastayesh S. "The comparative investigation and calculation of thermo-neutronic parameters on two gens II and III nuclear reactors with same powers," fuel. Vol. 100, pp. 60, 2011.

[6] Zankl M, Becker J, Fill U, Petoussi-Henss N, and Eckerman K.F. "GSF male and female adult voxel models representing ICRP Reference Man–the present status," The Monte Carlo Method: Versatility Unbounded in a Dynamic Computing World. vol. 1721, pp. 1-13, 2005.

[7] Eckerman KF, Update on ORNL RBE Work. ISCORS Meeting. 2011 Oak Ridge, USA.

[8] Ji S and Zhao W. "Displacement voxelization to resolve mesh-image mismatch: application in deriving dense white matter fiber strains,"

Computer methods and programs in biomedicine. vol. 213, pp.106528, 2022.

[9] Griffin KT, Cuthbert TA, Dewji SA, and Lee C. "Stylized versus voxel phantoms: a juxtaposition of organ depth distributions," Physics in Medicine & Biology. vol. 65, pp. 065007, 2020.

[10] Zaidi H and Xu XG. "Computational anthropomorphic models of the human anatomy: the path to realistic Monte Carlo modeling in radiological sciences," Annu. Rev. Biomed. Eng. vol. 9, pp. 471-500, 2007.

[11] Yan S and Fang Q. "Hybrid mesh and voxel based Monte Carlo algorithm for accurate and efficient photon transport modeling in complex bio-tissues," Biomedical Optics Express. vol. 11, pp. 6262-6270, 2020.

[12] Rajon D.A, Jokisch D.W, Patton P.W, Shah A.P, and Bolch W.E. "Voxel size effects in three‐dimensional nuclear magnetic resonance microscopy performed for trabecular bone dosimetry," Medical physics. vol. 27, pp. 2624-2635, 2000.

[13] Fisher Jr H.L and Snyder W.S, "Distribution of dose in the body from a source of gamma rays distributed uniformly in an organ," InProceedings of the First International Congress of Radiation Protection. vol. 1968 , pp. 1473-1486, 1968.

[14] Kramer R, Khoury H.J, Vieira J.W, Loureiro E.C, Lima V.J, and Lima F.R, "Hoff G. All about FAX: a Female Adult voXel phantom for Monte Carlo calculation in radiation protection dosimetry," Physics in Medicine & Biology. vol. 49, pp. 5203, 2004.

[15] IAEA-TECDOC-1223. Current status of neutron therapy. Austria (Vienna): International Atomic Energy Agency; 2001 May.

[16] Lee C, Lodwick D, Hasenauer D, Williams J.L, Lee C, and Bolch W.E. "Hybrid computational phantoms of the male and female newborn patient: NURBS-based whole-body models," Physics in Medicine & Biology. vol. 52, pp. 3309, 2007.

[17] Xu X.G, Taranenko V, Zhang J, and Shi C. "A boundary-representation method for designing whole-body radiation dosimetry models: pregnant females at the ends of three gestational periods—RPI-P3,-P6 and-P9," Physics in Medicine & Biology. vol. 52, pp. 7023, 2007.

[18] Zhang J, Na Y.H, Caracappa P.F, and Xu X.G. "RPI-AM and RPI-AF, a pair of mesh-based, size-adjustable adult male and female computational phantoms using ICRP-89 parameters and their calculations for organ doses from monoenergetic photon beams," Physics in Medicine & Biology. vol. 54, pp. 5885, 2009.

[19] Wambaugh J and Shah I. "A model for micro-dosimetry in virtual liver tissues," The 10th International Conference on Systems Biology Stanford, 2009.

[20] Stenvall A, Larsson E, and Strand S.E, "Jönsson BA. A small-scale anatomical dosimetry model of the liver," Physics in Medicine & Biology.vol. 59, pp. 3353, 2014.

[21] Yoon H, Lee S.K, Kim J.Y, and Joo M.W. "Quantitative Bone SPECT/CT of Central Cartilaginous Bone Tumors: Relationship between SUVmax and Radiodensity in Hounsfield Unit," Cancers. vol. 16, pp.1968, 2024.

[22] Hounsfield G.N. "Computed medical imaging," Science. vol. 210, pp. 22-28, 1980.

[23] Reeves T.E Mah P, and McDavid W.D. "Deriving Hounsfield units using grey levels in cone beam CT: a clinical application," Dentomaxillofacial radiology. vol. 41, pp.500-508, 2012.